

# Joint Optimization of Coded Illumination and Grayscale Conversion for One-Shot Raw Material Classification

Chao Wang  
c\_wang@pluto.ai.kyutech.ac.jp  
Takahiro Okabe  
okabe@ai.kyutech.ac.jp

Department of Artificial Intelligence  
Kyushu Institute of Technology  
Izuka, Fukuoka 820-8502, Japan

---

## Abstract

Classifying materials and their surface states is important for machine vision applications such as visual inspection. In this paper, we propose an approach to one-shot per-pixel classification of raw materials on the basis of spectral BRDFs; a surface of interest is illuminated by multispectral and multidirectional light sources at the same time. Specifically, we achieve two-class classification from a single color image; it directly finds the linear discriminant hyperplane with the maximal margin in the spectral BRDF feature space by jointly optimizing the non-negative coded illumination and the grayscale conversion. In addition, we extend our method to multiclass classification by exploiting the degree of freedom of the grayscale conversion. The experiments using an LED-based multispectral dome show that the performance of our proposed method with only a single image is better than or comparable to the state-of-the-art methods with multiple images.

## 1 Introduction

Classifying material categories such as metals and plastics, material themselves such as iron and aluminum, and their surface states such as rust, cracks, and scratches is important for machine vision applications such as recycling [22] and visual inspection of metallic surfaces [18, 26] and printed circuit boards [9, 23]. In this study, we focus on uncoated and unpainted raw materials, and achieve appearance-based material classification that works in a non-contact and non-destructive manner.

In general, the appearance of an object surface depends not only on the reflectance properties of the surface but also on the light sources illuminating it. Therefore, active illumination is often used for appearance-based material classification in order to extract discriminative features. The existing methods for material classification use a set of images taken under varying polarization states [8, 25], varying light source colors [9, 20], and varying light source directions [8, 24]. In particular, per-pixel material classification based on coded illumination [8, 13, 14], which uses images taken under multispectral and multidirectional light sources, has advantages that it exploits both the colors and directions of light sources, in other words spectral BRDFs, and requires only a small number of images, and has benefits in signal-to-noise ratio (SNR) due to illumination multiplexing.

Those methods based on coded illumination [6, 13, 14] optimize the intensities of multispectral and multidirectional light sources so that the images taken under those light sources are distinct. Unfortunately, however, they allow the optimal intensities to be negative, and as a result require two actual images taken under light sources with non-negative intensities; they consider the difference of the two images as the image taken under the optimal light sources with possibly negative intensities. Therefore, we cannot use those methods for objects in motion, *e.g.* ones on conveyor belt, because it is not easy to capture two images of moving objects with the same pose and from the same viewpoint but under different illumination conditions.

Accordingly, we propose an approach to *one-shot* per-pixel classification of raw materials on the basis of spectral BRDFs; a surface of interest is illuminated by multispectral and multidirectional light sources at the same time. Specifically, we achieve two-class classification from a single color image by incorporating the non-negativity constraints on light source intensities into optimization. In particular, our proposed method *directly* finds the linear discriminant hyperplane with the maximal margin in the spectral BRDF feature space by jointly optimizing the non-negative coded illumination and the grayscale conversion. In addition, we extend our method to multiclass classification by exploiting the degree of freedom of the grayscale conversion. We show that the optimization problems for the two-class and multiclass classifications result in alternative quadratic optimization problems.

To confirm the effectiveness of our proposed method, we conducted a number of experiments on a set of images of metals taken by using an LED-based multispectral dome similar to existing ones [10, 6, 12]. It consists of the clusters of light sources at different directions, and each cluster has LEDs with different spectral intensities. The experimental results show that the performance of our method with only a single image is better than or comparable to the state-of-the-art methods [6, 13] with multiple images.

The main contribution of this study is threefold. First, we achieve one-shot raw material classification that is applicable to objects in motion in contrast to the existing methods with multiple images. Second, we reveal the relationship among the coded illumination, the grayscale conversion, and the coefficients of a linear discriminant hyperplane in the spectral BRDF feature space. Then, our proposed method directly finds the linear discriminant hyperplane with the maximal margin by jointly optimizing the non-negative coded illumination and the grayscale conversion. Third, we extend our method to multiclass classification by exploiting the degree of freedom of the grayscale conversion. We show that the non-negative coded illumination and the grayscale conversion can jointly be optimized by using quadratic programming [16], and that our method with only a single image works better than or comparable to the state-of-the-art methods with multiple images.

## 2 Related Work

### 2.1 Active Illumination for Material Classification

In general, the reflected light observed on an object surface consists of a specular reflection component and a diffuse reflection component. It is known that the former is polarized whereas the latter is unpolarized, when we observe the reflected light from an object surface illuminated by polarized light. Wolff [25] and Chen and Wolff [8] studied those properties of specular and diffuse reflection components, and proposed polarization-based methods for classifying metals and dielectrics.

The reflectance of an object surface depends on the wavelength of light; the fraction of incident light power at each wavelength that is reflected on it is called spectral reflectance. Taking account of such a dependence of surface reflectance on wavelength, Salamati *et al.* [20] proposed material classification using color and NIR images, and Ibrahim *et al.* [6] proposed material classification and inspection based on spectral reflectance.

The roughness of an object surface is also a clue for classifying materials and their surface states. In more general, the reflectance property of an object surface depends not only on the direction of a viewpoint but also on the direction of a light source, and is described by a BRDF. Wang *et al.* [24] and Jehle *et al.* [8] proposed to optimize the light source directions for material classification based on BRDFs.

The above methods based on active illumination require a number of images taken under varying polarization states [9, 15], varying light source colors [7, 20], and varying light source directions [8, 24]. Therefore, those methods have difficulties in classifying materials of objects in motion. In contrast to them, our proposed method requires only a single image, and as a result is applicable to objects in motion.

## 2.2 Coded Illumination for Material Classification

Compared with the straightforward active illumination using a single light source, coded illumination using multiple light sources is efficient in terms of the number of required images and SNR. It is shown that coded illumination is effective for image acquisition [7, 19, 21], BRDF measurement [8], shape recovery [15] and spectral reflectance recovery [10, 17]. Whereas those methods optimize coded illumination for reconstructing signals with high SNR, our proposed method optimizes it for maximizing discriminative ability.

Gu and Liu [6] proposed an approach to per-pixel classification of raw materials based on spectral BRDFs. Specifically, they optimize the intensities of multispectral and multidirectional light sources for two-class classification via a linear SVM or Fisher LDA. Unfortunately, however, their method requires two grayscale images taken under actual light sources with non-negative intensities, since they allow the optimal intensities to be negative. They extended their method to multiclass classification by combining their two-class classifiers in a one-versus-one manner. Therefore, it requires  $[K(K-1)/2 + 1]$  grayscale images for  $K$ -class classification. In contrast to Gu and Liu [6], we incorporate the non-negativity constraints on light source intensities into optimization, and as a result our proposed method requires only a single image for both two-class and multiclass classifications. Therefore, our method is applicable to objects in motion.

Liu and Gu [13] extended the above methods using grayscale images to those using color images. Specifically, they optimize the intensities of multispectral and multidirectional light sources for dimensionality reduction of the spectral BRDF feature space. They use two-class or multiclass Fisher LDA and find the 3-D feature space that maximizes the ratio between the between-class scattering and the within-class scattering. We can combine their proposed method for dimensionality reduction with any classifiers, *e.g.* linear SVMs in the 3-D feature space. Unfortunately, however, their method requires two color images similar to the above. In contrast to Liu and Gu [13], our proposed method requires only a single color image for both two-class and multiclass classifications. In addition, our method directly finds the linear discriminant hyperplane with the maximal margin in the spectral BRDF feature space. The experimental results in Section 4 show that directly maximizing the margin in the original feature space works better than maximizing the margin in the 3-D feature space, *i.e.* Fisher LDA followed by linear SVMs.

### 3 Proposed Method

In this section, we propose an approach to per-pixel classification of raw materials from a single color image on the basis of spectral BRDFs. First, we show how RGB values observed under coded illumination are converted to a grayscale value, and reveal the relationship among the coded illumination, the grayscale conversion, and the coefficients of a linear discriminant hyperplane in the spectral BRDF feature space. Second, we present our proposed method for two-class classification that jointly optimizes the non-negative coded illumination and the grayscale conversion. Third, we extend our method to multiclass classification.

#### 3.1 Grayscale Value under Coded Illumination

Similar to the existing methods [6, 13], we assume that an object of interest is an opaque, unpainted, and planar surface and that its images under multispectral and multidirectional light sources are captured by using a single color camera. We make use of an LED-based multispectral dome; it has  $D$  clusters of light sources at different directions and each cluster has  $C$  LEDs with different spectral intensities, *i.e.*  $L (= C \times D)$  light sources in total.

The reflectance property of a point on an opaque surface is described by a spectral BRDF  $f(\theta_i, \phi_i, \theta_o, \phi_o, \lambda)$ , which is a 5-D function with respect to the direction of incident light  $(\theta_i, \phi_i)$ , the direction of reflected light  $(\theta_o, \phi_o)$ , and the wavelength  $\lambda$ . The above setup enables us to sample the spectral BRDFs on an object surface in both the angular domain of the incident light  $(\theta_i, \phi_i)$  and the spectral domain  $\lambda$ , when the LEDs are narrow-band and distant from the object surface. The  $L$ -D vectors  $\{\mathbf{x}_r, \mathbf{x}_g, \mathbf{x}_b\}$  consisting of the RGB values observed at a point on the object surface under the  $L$  light sources with unit intensities is called the *spectral BRDF feature* [6]. We consider a linear discriminant hyperplane in the  $3L$ -D feature space  $(\mathbf{x}_r^\top, \mathbf{x}_g^\top, \mathbf{x}_b^\top)^\top$  termed the spectral BRDF feature space.

Let us denote the coded illumination, *i.e.* the  $L$ -D vector consisting of the intensities of the  $L$  light sources by  $\mathbf{w} = (w_1, w_2, w_3, \dots, w_L)^\top$ . According to the superposition principle, the RGB values  $(I_r, I_g, I_b)^\top$  observed at the surface point under the coded illumination are given by the inner product between the spectral BRDF feature and the coded illumination as

$$\begin{pmatrix} I_r \\ I_g \\ I_b \end{pmatrix} = \begin{pmatrix} \mathbf{x}_r^\top \\ \mathbf{x}_g^\top \\ \mathbf{x}_b^\top \end{pmatrix} \mathbf{w}. \quad (1)$$

Then, the RGB values are converted to the grayscale value  $I$  by using the weights for the grayscale conversion  $\{w_r, w_g, w_b\}$  as

$$I = (w_r, w_g, w_b) \begin{pmatrix} I_r \\ I_g \\ I_b \end{pmatrix} \quad (2)$$

$$= (w_r, w_g, w_b) \begin{pmatrix} \mathbf{x}_r^\top \\ \mathbf{x}_g^\top \\ \mathbf{x}_b^\top \end{pmatrix} \mathbf{w} \quad (3)$$

$$= w_r \mathbf{w}^\top \mathbf{x}_r + w_g \mathbf{w}^\top \mathbf{x}_g + w_b \mathbf{w}^\top \mathbf{x}_b. \quad (4)$$

The above equation means that the grayscale value  $I$  is bilinear with respect to the coded illumination  $\mathbf{w}$  and the grayscale conversion  $\{w_r, w_g, w_b\}$ .

Thus, the grayscale value  $I$  that is converted from the RGB values observed under the coded illumination  $\mathbf{w}$  by using the weights for the grayscale conversion  $\{w_r, w_g, w_b\}$  gives the linear discriminant hyperplane in the  $3L$ -D spectral BRDF feature space:

$$I + b = w_r \mathbf{w}^\top \mathbf{x}_r + w_g \mathbf{w}^\top \mathbf{x}_g + w_b \mathbf{w}^\top \mathbf{x}_b + b = 0, \quad (5)$$

where  $b$  is the bias term. In contrast to usual linear discriminant hyperplanes, the  $3L$  coefficients of the hyperplane in eq.(5) depend on each other, because the contribution of the coded illumination is common to the RGB channels but the weights for the grayscale conversion differ from one channel to another.

## 3.2 Two-Class Classification from a Single Image

We jointly optimize the non-negative coded illumination  $\mathbf{w}$  and the grayscale conversion  $\{w_r, w_g, w_b\}$  in eq. (5) via margin maximization. Specifically, similar to soft margin SVMs [4], the optimization problem is formulated as

$$\min_{\mathbf{w}, w_r, w_g, w_b, b, \xi_n} \left[ \frac{1}{2} |\mathbf{w}|^2 (w_r^2 + w_g^2 + w_b^2) + \alpha \sum_{n=1}^N \xi_n \right] \quad (6)$$

$$\text{subject to} \quad y_n [\mathbf{w}^\top (w_r \mathbf{x}_{nr} + w_g \mathbf{x}_{ng} + w_b \mathbf{x}_{nb}) + b] \geq 1 - \xi_n \quad (n = 1, 2, 3, \dots, N), \quad (7)$$

$$\xi_n \geq 0 \quad (n = 1, 2, 3, \dots, N), \quad (8)$$

$$w_l \geq 0 \quad (l = 1, 2, 3, \dots, L). \quad (9)$$

Here,  $(\mathbf{x}_{nr}^\top, \mathbf{x}_{ng}^\top, \mathbf{x}_{nb}^\top)^\top$ ,  $y_n$ , and  $\xi_n$  are the spectral BRDF feature, the label, and the slack variable of the  $n$ -th training sample respectively.  $N$  and  $\alpha$  are the number of training samples and the weight for the penalty term. Thanks to the non-negativity constraints in eq.(9), our proposed method can directly find the linear discriminant hyperplane with the maximal margin in the spectral BRDF feature space from a single color image taken under the optimal non-negative coded illumination followed by the optimal grayscale conversion. Note that the weights for the grayscale conversion  $\{w_r, w_g, w_b\}$  can be negative, since the conversion from RGB to grayscale is post-processing.

The above optimization problem cannot be solved in a similar manner to soft margin SVMs, since the  $3L$  coefficients of the linear discriminant hyperplane in eq.(5) depend on each other as described before. However, when one of the coded illumination and the grayscale conversion is fixed, it results in the quadratic optimization problem with respect to the other. Therefore, we use an alternative optimization technique. Specifically, we set the initial condition as  $\mathbf{w} = (1, 1, 1, \dots, 1)^\top$  and  $b = 1$ , and then update the grayscale conversion  $\{w_r, w_g, w_b\}$  and the set of the coded illumination and the bias  $\{\mathbf{w}, b\}$  alternatively by using the quadratic programming.

## 3.3 Extension to Multiclass Classification from a Single Image

In order to extend our proposed method to multiclass classification from a single image, we exploit the degree of freedom of the grayscale conversion. Specifically, even though the coded illumination  $\mathbf{w}$  under which a single image of an object surface is taken is fixed, we can obtain  $M$  linear discriminant hyperplanes:

$$w_{mr} \mathbf{w}^\top \mathbf{x}_r + w_{mg} \mathbf{w}^\top \mathbf{x}_g + w_{mb} \mathbf{w}^\top \mathbf{x}_b + b_m = 0 \quad (10)$$

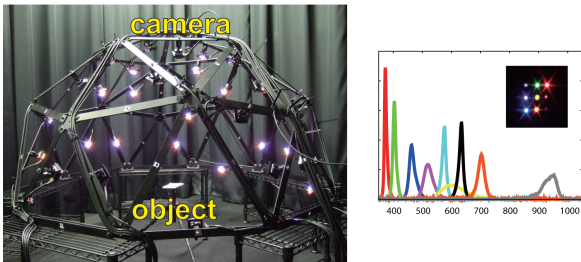


Figure 1: Our LED-based multispectral dome termed Kyutech Light Stage I. It consists of LED clusters, each of which has LEDs with different spectral intensities.

by changing the weights for the grayscale conversions  $\{w_{mr}, w_{mg}, w_{mb}\}$  ( $m = 1, 2, 3, \dots, M$ ) according to materials to be classified. Here,  $M = K(K - 1)/2$  for  $K$ -class classification when combining binary classifiers in a one-versus-one manner, and  $b_m$  is the bias term for the  $m$ -th linear discriminant hyperplane.

Similar to the case of our two-class classification, we jointly optimize the non-negative coded illumination  $\mathbf{w}$  and the grayscale conversions  $\{w_{mr}, w_{mg}, w_{mb}\}$  via margin maximization. Specifically, the optimization problem for the multiclass classification is formulated as

$$\min_{\mathbf{w}, w_{mr}, w_{mg}, w_{mb}, b_m, \xi_{mn}} \left[ \sum_{m=1}^M \frac{1}{2} |\mathbf{w}|^2 (w_{mr}^2 + w_{mg}^2 + w_{mb}^2) + \alpha \sum_{m=1}^M \sum_{n=1}^N \xi_{mn} \right] \quad (11)$$

$$\text{subject to} \quad y_n [\mathbf{w}^\top (w_{mr} \mathbf{x}_{nr} + w_{mg} \mathbf{x}_{ng} + w_{mb} \mathbf{x}_{nb}) + b_m] \geq 1 - \xi_{mn} \quad (12)$$

$$(n = 1, 2, 3, \dots, N; \quad m = 1, 2, 3, \dots, M),$$

$$\xi_n \geq 0 \quad (n = 1, 2, 3, \dots, N), \quad (13)$$

$$w_l \geq 0 \quad (l = 1, 2, 3, \dots, L). \quad (14)$$

We solve the above optimization problem by using an alternative optimization technique in a similar manner to our two-class classification. Specifically, we set the initial condition as  $\mathbf{w} = (1, 1, 1, \dots, 1)^\top$ , and then update the set of the grayscale conversions and the biases  $\{w_{mr}, w_{mg}, w_{mb}, b_m\}$  and the coded illumination  $\mathbf{w}$  alternatively by using the quadratic programming.

## 4 Experiments

### 4.1 Experimental Setup

We tested raw materials with very similar appearance, specifically seven iron plates: SECC, SEHC, SGCC, SGHC, SPCC, SPHC-P, and ZAM. This is because we found in our preliminary experiments that material classification based on spectral BRDFs works well for materials with different object colors. Figure 2 (a) shows the images of those materials under the same illumination condition.

We illuminated objects of interest by using our LED-based multispectral dome termed Kyutech Light Stage I [9, 10] in Figure 1. It consists of the clusters of light sources at

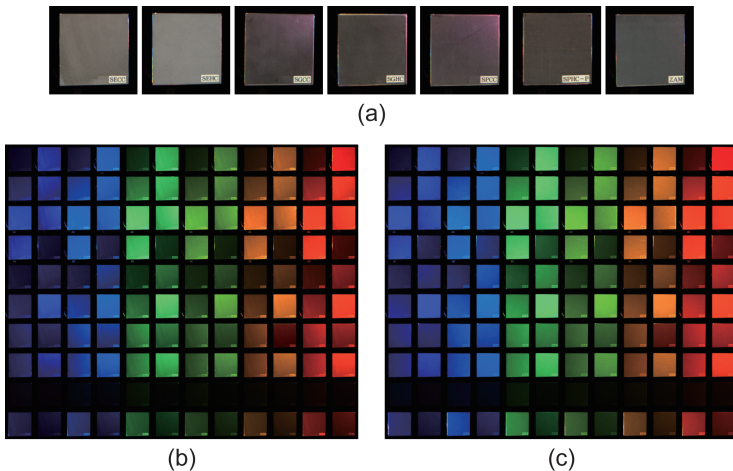


Figure 2: Materials tested in our experiments: (a) seven iron plates: SECC, SEHC, SGCC, SGHC, SPCC, SPHC-P, and ZAM from left to right, (b) the images of SECC under 120 multispectral and multidirectional light sources, and (c) those of SEHC.

different directions on the dome with the diameter of 1.5 m, and each cluster has LEDs with different spectral intensities. Figure 2 (b) and (c) show the images of SECC and SEHC captured by using a Point Grey Flea3 camera with a linear radiometric response function under 120 ( $= L$ ) light sources; 6 ( $= C$ ) colors  $\times$  20 ( $= D$ ) directions. The peak wavelengths of those LEDs are 405, 464, 523, 573, 601, and 630 nm respectively. The images used in our experiments will be made publicly available <sup>1</sup>.

We trained classifiers by using such 120 images per material. We used the pixel values at an area of  $50 \times 50$  pixels on an object surface for training and those at the other area of  $50 \times 50$  pixels for test. Note that the pixel values of each surface are not the same even under the same illumination condition due to nonuniform finish and fine scratches. The weight for the penalty term  $\alpha$  in eq.(6) and eq.(11) was determined by using the training samples. We used the MATLAB implementation of the interior-point-convex algorithm for optimization. We confirmed that the alternative optimization converges within 10 to 15 iterations.

## 4.2 Two-Class Classification

To confirm the effectiveness of our proposed method for two-class classification, we compared the performance of our method with those of the following methods.

- **Gu and Liu [6]:** This method requires two grayscale images. Our method from eq.(6) to eq.(9) results in it, when the grayscale conversion is fixed, *e.g.*  $w_r = w_g = w_b = 1/3$  in this paper, and the non-negativity constraints in eq.(9) are removed.
- **Gu and Liu [6] with non-negativity constraints:** This method requires only a single grayscale image. We incorporate the non-negativity constraints on light source inten-

<sup>1</sup>Because the dataset of raw material images used in [6] is not available currently, we prepared our own dataset.

Method	Required Images	Classification Rate
Our proposed method	single color	99.95%
Gu and Liu [6]	two grayscale	99.98%
Gu and Liu [6] with non-negativity constraints	single grayscale	97.82%
Liu and Gu [13] with a linear SVM	two color	99.12%

Table 1: Results for two-class classification.

sities into Gu and Liu [6] for comparison. Our method from eq.(6) to eq.(9) results in it, when the grayscale conversion is fixed, *e.g.*  $w_r = w_g = w_b = 1/3$  in this paper.

- **Liu and Gu [13] with a linear SVM:** This method requires two color images. We combine Liu and Gu [13], which reduces the dimensionality of the feature space from  $3L$  to 3 by using Fisher LDA, with a linear SVM in the 3-D feature space for comparison. Specifically, in eq.(5), the coded illumination  $\mathbf{w}$  is computed via Fisher LDA and the weights for the grayscale conversion  $\{w_r, w_g, w_b\}$  are computed via a linear SVM.

We conducted two-class classification for all the combinations of the 7 materials, *i.e.* 21 ( $= {}_7C_2$ ) combinations in total. Table 1 shows the classification rate for each method averaged over the all combinations. First, we can see that our proposed method performs comparable to Gu and Liu [6], even though ours requires not two images but only a single image. Second, we can see that our method works better than Gu and Liu [6] with non-negativity constraints on light source intensities. This shows the effectiveness of using color image and optimizing the grayscale conversion. Third, the performance of our method is better than that of Liu and Gu [13] with a linear SVM, even though ours requires only a single image. This shows the advantage of directly finding the linear discriminant hyperplane with the maximal margin in the  $3L$ -D feature space over the sequential optimization, *i.e.* the dimensionality reduction from  $3L$  to 3 by using Fisher LDA followed by a linear SVM in the 3D feature space.

Figure 3 shows some of the coded illuminations obtained by using our proposed method and the other methods for 4 two-class classifications: (a) SECC vs. SGCC, (b) SGCC vs. SPCC, (c) SGHC vs. ZAM, and (d) SEHC vs. SPHC-P. First, we can see that the coded illuminations of our proposed method (the 4th row) is similar in some degree to those of Gu and Liu [6] with non-negativity constraints (the 2nd row) and the positive or negative halves of Gu and Liu [6] (the 1st row). Second, as shown in (d), the coded illumination obtained by using Gu and Liu [6] can have only non-negative intensities by accident without imposing the non-negativity constraints. Third, more interestingly, the coded illuminations obtained by using Liu and Gu [13] (the 3rd row), *i.e.* Fisher LDA are very different from those by using our method based on margin maximization.

### 4.3 Multiclass Classification

To confirm the effectiveness of our proposed method for multiclass classification, we compared the performance of our method with those of the following methods.

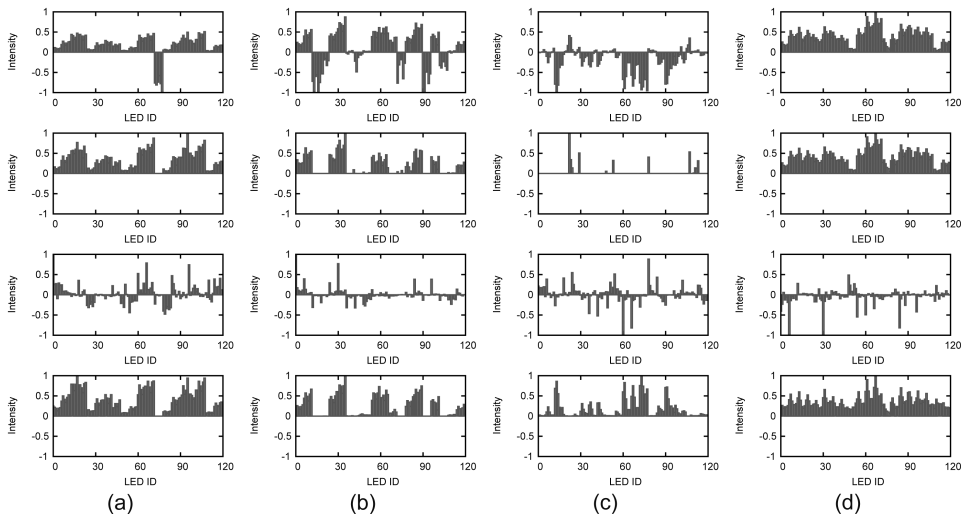


Figure 3: From top to bottom, the coded illuminations obtained by using Gu and Liu [6], Gu and Liu [6] with non-negativity constraints, Liu and Gu [13], and our proposed method for (a) SECC vs. SGCC, (b) SGCC vs. SPCC, (c) SGHC vs. ZAM, and (d) SEHC vs. SPHC-P.

Method	Required Images	Classification Rate
Our proposed method	single color	99.54%
Gu and Liu [6]	seven grayscale	99.95%
Liu and Gu [13] with linear SVMs	two color	82.51%

Table 2: Results for multiclass classification.

- **Gu and Liu [6]:** This method requires  $\lceil K(K-1)/2 + 1 \rceil$  grayscale images for  $K$ -class classification, since it combines their binary classifiers described in the previous section in a one-versus-one manner<sup>2</sup>.
- **Liu and Gu [13] with linear SVMs:** This method requires two color images. We combine Liu and Gu [13], which reduces the dimensionality of the feature space from  $3L$  to 3 by using multiclass Fisher LDA, with linear SVMs in the 3-D feature space for comparison. Specifically, in eq.(10), the coded illumination  $\mathbf{w}$  is computed via Fisher LDA and the grayscale conversions  $\{w_{rm}, w_{gm}, w_{bm}\}$  are computed via linear SVMs.

We conducted four-class classification ( $K = 4$ ) for all the combinations of the 7 materials, *i.e.* 35 ( $= 7C_4$ ) combinations in total. Table 2 shows the classification rate for each method averaged over the all combinations. First, compared with Gu and Liu [6], we can see that the

<sup>2</sup>Note that the multiclass classification based on Gu and Liu [6] with non-negativity constraints, *i.e.* the combination of their binary classifiers described in the previous section requires not a single image but  $\lceil K(K-1)/2 \rceil$  images. It is clear that its performance is worse than that of our proposed method in Table 2.

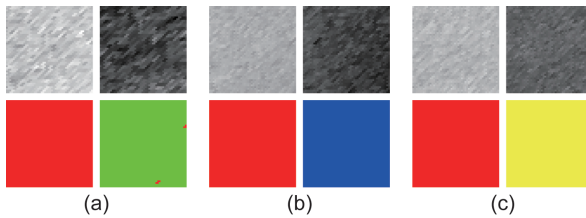


Figure 4: The grayscale images (top) and the classification results (bottom): (a) SECC vs. SEHC, (b) SECC vs. SGCC, and (c) SECC vs. SGHC.

degradation in classification rate of our proposed method is minor even though our method reduces the required number of images from seven to one. Second, the performance of our method is better than that of Liu and Gu [13] with linear SVMs, even though ours requires not two images but only a single image. This clearly shows the advantage of directly finding the linear discriminant hyperplanes with the maximal margins in the spectral BRDF feature space over the sequential optimization, *i.e.* the dimensionality reduction followed by linear SVMs in the 3D feature space.

Figure 4 shows some of the grayscale images (top) converted from color images under the optimal coded illumination by using the optimal grayscale conversions, and the classification results (bottom). Here, red, green, blue, and yellow stand for SECC, SEHC, SGCC, and SGHC respectively. We can see that the grayscale images are distinct each other even though the color images are captured under the same illumination condition.

## 5 Conclusion and Future Work

In this paper, we proposed an approach to one-shot per-pixel classification of raw materials on the basis of spectral BRDFs. Specifically, we reveal the relationship among the coded illumination, the grayscale conversion, and the coefficients of a linear discriminant hyperplane in the spectral BRDF feature space, and then directly find the linear discriminant hyperplane with the maximal margin by jointly optimizing the non-negative coded illumination and the grayscale conversion. In addition, we extend our method to multiclass classification by exploiting the degree of freedom of the grayscale conversion. We conducted the experiments using an LED-based multispectral dome and confirmed that our method with only a single image works better than or comparable to the state-of-the-art methods with multiple images.

The future work of this study includes the extension to complex objects such as non-planar surfaces, textured surfaces [14], translucent materials, and fluorescent materials. The extension to non-linear classifiers is another direction of our future work.

## Acknowledgments

This work was partially supported by JSPS KAKENHI Grant Numbers JP17H01766 and JP16H01676.

## References

- [1] B. Ajdin, M. Finckh, C. Fuchs, J. Hanika, and H. Lensch. Compressive higher-order sparse and low-rank acquisition with a hyperspectral light stage, 2012. Technical Report, Eberhard Karls Universität Tübingen, WSI-2012-01.
- [2] M. Alterman, Y. Schechner, and A. Weiss. Multiplexed fluorescence unmixing. In *Proc. IEEE ICCP2010*, pages 1–8, 2010.
- [3] H. Chen and L. Wolff. Polarization phase-based method for material classification in computer vision. *IJCV*, 28(1):73–83, 1998.
- [4] C. Cortes and V. Vapnik. Support-vector networks. *Machine Learning*, 20(3):273–297, 1995.
- [5] A. Ghosh, S. Achutha, W. Heidrich, and M. O’Toole. BRDF acquisition with basis illumination. In *Proc. IEEE ICCV2007*, pages 1–8, 2007.
- [6] J. Gu and C. Liu. Discriminative illumination: per-pixel classification of raw materials based on optimal projections of spectral BRDF. In *Proc. IEEE CVPR2012*, pages 797–804, 2012.
- [7] A. Ibrahim, S. Tominaga, and T. Horiuchi. Spectral imaging method for material classification and inspection of printed circuit boards. *Optical Engineering*, 49(5):057201, 2010.
- [8] M. Jehle, C. Sommer, and B. Jähne. Learning of optimal illumination for material classification. In *Proc. DAGM2010*, pages 563–572, 2010.
- [9] M. Kitahara, T. Okabe, C. Fuchs, and H. Lensch. Simultaneous estimation of spectral reflectance and normal from a small number of images. In *Proc. VISAPP2015*, pages 303–313, 2015.
- [10] N. Kobayashi and T. Okabe. Separating reflection components in images under multispectral and multidirectional light sources. In *Proc. ICPR2016*, pages 3210–3215, 2016.
- [11] A. Lam, A. Subpa-Asa, I. Sato, T. Okabe, and Y. Sato. Spectral imaging using basis lights. In *Proc. BMVC2013*, 2013.
- [12] C. LeGendre, X. Yu, D. Liu, J. Busch, A. Jones, S. Pattanaik, and P. Debevec. Practical multispectral lighting reproduction. 35(4):Article No.32, 2016.
- [13] C. Liu and J. Gu. Discriminative illumination: per-pixel classification of raw materials based on optimal projections of spectral BRDF. *IEEE Trans. PAMI*, 36(1):86–98, 2014.
- [14] C. Liu, G. Yang, and J. Gu. Learning discriminative illumination and filters for raw material classification with optimal projections of bidirectional texture functions. In *Proc. IEEE CVPR2013*, pages 1430–1437, 2013.
- [15] W.-C. Ma, T. Hawkins, P. Peers, C.-F. Chabert, M. Weiss, and P. Debevec. Rapid acquisition of specular and diffuse normal maps from polarized spherical gradient illumination. In *Proc. EGSR2007*, pages 183–194, 2007.

- [16] J. Nocedal and S. Wright. *Numerical Optimization*. Springer New York, ISBN: 978-0-387-30303-1, 2006.
- [17] J.-I. Park, M.-H. Lee, M. Grossberg, and S. Nayar. Multispectral imaging using multiplexed illumination. In *Proc. IEEE ICCV2007*, pages 1–8, 2007.
- [18] F. Pernkopf and P. O’Leary. Image acquisition techniques for automatic visual inspection of metallic surfaces. *NDT&E International*, 36:609–617, 2003.
- [19] N. Ratner and Y. Schechner. Illumination multiplexing within fundamental limits. In *Proc. IEEE CVPR2007*, pages 1–8, 2007.
- [20] N. Salamati, C. Fredembach, and S. Stsstrunk. Material classification using color and NIR images. In *Proc. IS&T/SID CIC2009*, 2009.
- [21] Y. Schechner, S. Nayar, and P. Belhumeur. A theory of multiplexed illumination. In *Proc. IEEE ICCV2003*, pages 808–815, 2003.
- [22] D. Scott. A two-colour near-infrared sensor for sorting recycled plastic waste. *Measurement Science and Technology*, 6(2):156–159, 1995.
- [23] S. Tominaga and S. Okamoto. Reflectance-based material classification for printed circuit boards. In *Proc. IEEE ICIAP2003*, pages 238–244, 2003.
- [24] O. Wang, P. Gunawardane, S. Scher, and J. Davis. Material classification using BRDF slices. In *Proc. IEEE CVPR2009*, pages 2805–2811, 2009.
- [25] L. Wolff. Polarization-based material classification from specular reflection. *IEEE Trans. PAMI*, 12(11):1059–1071, 1990.
- [26] H. Zheng, L. Kong, and S. Nahavandi. Automatic inspection of metallic surface defects using genetic algorithms. *Journal of Materials Processing Technology*, 125–126:427–433, 2002.